# The fcc solid solution stability in the Co-Cr-Fe-Mn-Ni multi-component system

Guillaume Bracq, Mathilde Laurent-Brocq, Loïc Perrière, Rémy Pirès, Jean-Marc Joubert, Ivan Guillot

# The fcc solid solution stability in the Co-Cr-Fe-Mn-Ni multi-component system

Guillaume Bracq, Mathilde Laurent-Brocq, Loïc Perrière, Rémy Pirès, Jean-Marc Joubert, Ivan Guillot

*Université Paris Est, ICMPE (UMR 7182), CNRS, UPEC, F-94320 Thiais France*

**Abstract**

The phase stability of the fcc solid solution in the Co-Cr-Fe-Mn-Ni system was theoretically and experimentally investigated. Using the Calphad approach and a new database (TCHEA1) devoted to high entropy alloys (HEA), the stable phases of 10 626 compositions could be calculated, depending on the temperature. 11 alloys were also processed and characterized. The comparison between calculations and experimental results indicates that the fcc solid solution is accurately described by the TCHEA1 database but, the $\sigma$ phase is more stable than the calculation predictions. It was shown that the fcc phase is stable over a wide range of compositions, which was completely described. Now it is possible to choose *a priori* a composition which will form a solid solution within the Co-Cr-Fe-Mn-Ni system. Finally, it was proven that Cr and Mn destabilize the fcc solid solution, unlike Ni and Co.

*Keywords:* Multi-component alloys, High entropy alloys, Solid solution, Calphad, Thermodynamic stability

## 1. Introduction

For a long time, development of alloys was restricted to one principal element, or rarely two, with minor elements added for properties and performances optimization. In 2004 [1, 2], an equimolar Cr, Mn, Fe, Co and Ni alloy was produced and was unexpectedly found to be single-phase. A new concept of materials was born: multi-component alloys forming a solid-solution and in which all components are very concentrated. By definition, this new material concept should make it possible to explore an almost infinite field of chemical compositions. Thus one of the expected advantage of this new concept was the possibility to more easily adjust properties through wide composition variations [3].

From a thermodynamic point of view, Yeh *et al.* [2] pointed out a critical role of the configurational entropy to stabilize the multi-component solid solutions and proposed the name high entropy alloys. Based on this statement, HEA were defined as alloys containing at least 5 elements in equimolar proportions, or with atomic concentrations between 5 and 35 at. % [4]. However several phases are formed for some alloys whose configurational entropy is nevertheless high [5, 6]. Maximizing configurational entropy is not enough to form a HEA. Indeed, phase formation is thermodynamically controlled by the variation of the mixing Gibbs free energy, $\Delta G_{mix}$, which is defined by: $\Delta G_{mix} = \Delta H_{mix} - T\Delta S_{mix}$, where $\Delta H_{mix}$, $\Delta S_{mix}$ and $T$ are respectively the enthalpy of mixing, the entropy of mixing and the temperature at which elements are mixed. It is mentioned that the term $\Delta S_{mix}$ includes all entropy sources, such as configuration, vibrational, electronic and magnetic contributions. The phase stability depends on the minimization of the Gibbs free energy and thus it is determined by the competition between $\Delta H_{mix}$ and $T\Delta S_{mix}$.

To better take into account the Gibbs free energy minimization, some empirical models based on the Hume-Rothery rules consider the differences of atomic size and of electronegativities, the electron-to-atom ratio together with $\Delta H_{mix}$ and $\Delta S_{mix}$ values, which were derived from binary alloys data [7, 8]. However, these models were proven not to be predictive [6]. Thus, it is not possible to determine *a priori* if a given composition will form a unique solid solution. One of the expected HEA advantage cannot be exploited. Instead, the study of non equimolar alloys has been restricted up to now to few compositions such as $Fe_{40}Mn_{27}Ni_{26}Co_5Cr_2$ [9] or $Fe_{40}Mn_{40}Co_{10}Cr_{10}$ [10].

*Corresponding author
*Email address:* laurent-brocq@icmpe.cnrs.fr (Mathilde Laurent-Brocq)

In this context, the objective of this study is to fully determine the composition range of existence of a unique solid solution within the multi-component Co-Cr-Fe-Mn-Ni system. To address this problem, it is decided to use the Calphad method. Indeed this method has already been applied to HEA and, although few compositions [11] or only equimolar alloys [12] were studied, the results were promising. Moreover, the TCHEA1 database, which was recently developed for high entropy alloys, was used. In order to evaluate the predictive character of calculated results, several alloys were processed and characterized.

## 2. Methods

### *2.1. Simulation method*

The Calphad approach has been chosen to calculate the quinary phase diagram of the Co-Cr-Fe-Mn-Ni system. The Calphad method relies on a self-consistent description of Gibbs energy for each phase of a system. This description is made thanks to semi-empirical functions, which depend on temperature and composition and which are optimized on reliable experimental phase diagram and thermodynamic data and DFT results. Those semi-empirical equations and the corresponding fitting parameters are called a database. Once a database has been developed, it can be used to calculate not only phase diagrams but also other thermodynamic properties. The limiting step in this context is the availability of a reliable thermodynamic database able to predict phase diagrams and thermodynamic properties of multi-component systems. Thermo-Calc has recently introduced a new database dedicated to HEA : TCHEA1 [13]. Contrary to other databases centered on one element for which the calculation should be limited to certain amount of alloying element, this database can, in principle, be used for any composition. TCHEA1 includes 15 elements and 163 phases whereas the system Co-Cr-Fe-Mn-Ni is decribed with 38 phases.

It has to be kept in mind that, in the Calphad method, high order phase diagram are extrapolated from lower order systems. So a precise description of the binary and ternary systems is required in order to obtain a reliable description of quaternary and quinary systems. The 10 binary phase diagrams of the Co-Cr-Fe-Mn-Ni system have been calculated with TCHEA1 and checked to reproduce the available literature data. This is, for example, not the case for Fe-Mn system in the steel database TCFE7 which does not consider $\alpha$ and $\beta$ Mn phases (see Supplementary Material 1).

Thus, for the Co-Cr-Fe-Mn-Ni system, it is preferable to use the TCHEA1 database rather than the TCFE7. However, in the TCHEA1 database, only 5 ternary diagrams have been optimized on experimental data while the 5 others were only extrapolated from binary systems. Thus an assessment of the TCHEA1 database is needed (see section 4.1).

First, the objective was to qualitatively show the role of each element (i.e.: Co, Cr, Fe, Mn and Ni). So five isopleths were plotted using the TCHEA1 database. The principle is to vary the atomic composition of one element (from 0 to 100%) while retaining the other elements in equimolar proportion. For example the equation that controls the alloy composition for the Co-isopleth can be written as follows : $\mathrm{Co}_x\mathrm{Cr}_{\frac{1-x}{4}}\mathrm{Fe}_{\frac{1-x}{4}}\mathrm{Mn}_{\frac{1-x}{4}}\mathrm{Ni}_{\frac{1-x}{4}}$. Second, in order to describe the whole Co-Cr-Fe-Mn-Ni quinary phase diagram, the stable phases were calculated at 1273 and 1373 K by varying the composition of each element by step of 5%. This represents 10 626 compositions among which 3876 quinaries, 4845 quaternaries, 1710 ternaries and 190 binaries.

### *2.2. Materials and experimental methods*

All alloys were prepared with the same procedure. A mixture of Co, Cr, Fe, Mn and Ni metals with purity exceeding 99.9 wt.% was used. To remove traces of oxides, mechanical polishing was performed on raw metals before the melting process. These alloys were produced by high frequency electromagnetic induction melting in a water-cooled copper crucible under He atmosphere. Then gravity casting was performed to shape the ingots. The cooling rate was estimated to be about $10^3 K.s^{-1}$ and a rod with a diameter of 13 mm and a length of around 8 cm was obtained. The rods were cut into slices of around 2-3 mm of length then cut in half. Finally the samples, which were wrapped in a tantalum sheet, were annealed at 1373 K for 6 days in a sealed silica tube filled with Ar atmosphere. Several alloys were also annealed at 1273 K for 2 or 6 days. After annealing, the samples were quickly cooled down. Thanks to this last processing step, it is assumed that the studied alloys represent the high temperature stable state. Samples were prepared by mechanical grinding using 1200 to 4000 grit SiC papers followed by a final polishing step using a vibratory table and a 0.04 micron colloidal silica for a minimum of 15h.

The samples were characterized by X-ray diffraction (XRD) with a PANalytical XPert Pro diffractometer using the Co-K$\alpha$ radiation at a wavelength of 0.178897 nm. Rietveld refinements were performed on all X-ray diffractograms (FullProf software) and used to determine the lattice parameters [14]. A Merlin Zeiss microscope was used for Scanning Electron Microscopy (SEM). The chemical composition was measured thanks to energy dispersive spectroscopy (EDS). Maps of each element were recorded. A minimum of 15 randomly distributed measurement points were also recorded for each phase. The given compositions and the corresponding uncertainties are respectively the average and the standard deviations of those measurements. Electron backscatter diffraction (EBSD) measurements were performed using Aztec HKL Advanced Nordlys Nano system (Oxford Instruments) at an acceleration voltage of 20 kV.

## 3. Results

### *3.1. Calphad calculations*

#### *3.1.1. Isopleths*

Isopleths based on the TCHEA1 database are depicted on figure 1. A dashed line representing equimolar CoCrFeMnNi alloy is plotted on all subfigures. This composition is a single-phase solid solution at high temperature as expected. For low temperatures, it can be observed that many phases coexist. This points the role of enthalpy whose influence is increasing when temperature decreases. This study will focus on phase stability for T > 1000 K because most literature data on HEA has been obtained at high temperature [11]. For these temperatures, the homogeneity range of fcc solid solution appears to extend widely in all isopleths. More precisely, on figure 1-a, CrFeMnNi quaternary equimolar alloy (left of the diagram) is two-phase (i.e. fcc + bcc). When adding Co, the bcc phase disappears and the system becomes a single fcc solid solution. For T > 1200 K, the fcc solid solution extends from 5 to 100 at. % Co. At lower temperatures, the domain of existence of a unique fcc solid solution is restricted by the appearance of the $\sigma$ phase, then, when increasing the Co content, by a bcc phase and finally by a miscibility gap between ferromagnetic and paramagnetic phases. The Ni-isopleth (figure 1-e) is similar to the Co-isopleth. However the temperature range of the fcc solid solution is larger than for Co. On the Fe-isopleth (figure 1-c), the unique fcc solid solution covers the entire range of composition for a large range of temperature, including the CoCrMnNi quaternary equimolar alloy. On the contrary, the range of existence of the fcc solid solution is more restricted on the Mn-isopleth (figure 1-d). Indeed the CoCrFeNi quaternary equimolar alloy is a unique fcc solid solution and the alloy remains single-phase up to 80 at. % Mn. For larger contents of Mn, the $\beta$-Mn phase is also formed. At lower temperatures, the single-phase field is restricted by the formation of either a bcc or a $\sigma$ phase. Finally, the Cr-isopleth (figure 1-b) can be compared to the Mn-isopleth with a more restricted domain of existence of the unique fcc solid solution. Indeed, at 1200K, for [Cr] > 28 at. %, bcc and fcc phases coexist and for [Cr] > 85 at. %, the fcc phase disappears.

Thus the five elements can be classified into 3 groups according to their influence on the stability of the unique fcc solid solution. First, Co and Ni favor its formation. Indeed the fcc solid solution exists in a very wide range of composition reaching the pure metals but when the Co or Ni content is too low, a second phase is formed. Second, Fe appears to have no significant effect. Indeed the fcc solid solution is stable from CoCrMnNi to pure Fe. Finally, Mn and even more Cr penalize the stability of the fcc solid solution, formed when they are absent and, which disappears if their content is too high. It has to be kept in mind that isopleths describe only alloys with four elements in equimolar proportions. In a second step, the whole range of possible compositions of the quinary Co-Cr-Fe-Mn-Ni system is systematically studied.

#### *3.1.2. Quinary section*

By varying the composition of each element from 0 to 100 at.% by 5 at.% step, 10 626 compositions were computed. Over 68% of the calculated alloys, that is to say 7282 and 7252 compositions at 1273 and 1373 K, respectively, form a unique fcc solid solution (table 1). So the composition range of existence of a unique solid solution is very wide for the Co-Cr-Fe-Mn-Ni system. More precisely, the percentage of compositions forming a unique fcc solid solution increases with the number of element (table 1). For example, at 1273 K, 45.8 and 73.1 % form a unique fcc solid solution in binary and quinary system, respectively. It can be noted that the results at 1273 or 1373 K are very similar.

These results can also be compared to the early HEA definition. Indeed HEA were defined by Yeh *et al.* [4] as any system composed of at least five elements with concentration between 5 and 35 at. %. 1670 alloys among the 3876 quinary alloys follow this definition (43.1%). However, only 1285 out of these 1670 (76.9%) form a unique fcc solid solution. On the contrary, 5997 alloys form a unique fcc solid solution but are not considered as HEA according to Yeh *et al.* definition. Thus this definition appears as not specific enough to describe multi-component solid solutions.

The average concentration of each element for all alloys whose stable phase is not a unique fcc solid solution was calculated. It can be noticed that the average Cr content is high (40 at.%) whereas Co and Ni contents are low (10 at.%). Thus adding a high concentration of Cr destabilizes the fcc solid solution. This is consistent with previous results obtained from isopleths.

Now, the objective is to graphically represent all the calculated data in order to map the range of existence of the unique fcc solid solution. It is challenging to represent a quinary phase diagram, or in other words a function of 5 independent variables. It is proposed to fix the temperature and to plot a matrix of quasi-ternary diagrams (figure 2). Since Cr and Mn were identified as elements which destabilize the solid solution, it was chosen to highlight their effect. Thus, for one given quasi-ternary diagram, the Cr and Mn contents are fixed and the stable phases are indicated as a function of Fe and Co contents. The Ni content cannot be read directly on the plot but it can be deduced thanks to the following equation: [Ni]=1-[Co]-[Cr]-[Fe]-[Mn]. It is mentioned that this specific representation is not unique. Based on the same principle, the role of Ni and Co, which stabilize the fcc solid solution could be highlighted and quasi-ternary diagrams could be plotted varying Fe and Cr contents (see Supplementary Material 2).

First, the quinary section confirms and generalizes the influence of each element on the stability of the unique fcc solid solution which was already approached by studying the isopleths. Especially, the destabilizing influence of Cr is clear. No composition with more than 50 at.% of Cr has a single fcc phase. Second, combined effects can be observed. The destabilizing role of Cr is magnified when adding Mn. Indeed, with 30 at. % of Mn, the content of Cr cannot exceed 30 at. % (in comparison with 50 at. % without Mn) to have the possibility to form a unique fcc solid solution (figure 2, line 4 and column 4).In presence of Cr, increasing Fe content is also detrimental to the fcc solid solution stability. Indeed, to form a unique fcc solid solution, the Fe content cannot exceed 40 or 20 at. % in the presence of 30 and 40 at. % Cr, respectively (figure 2, line 0 and columns 4 and 5). It can be explained by the fact that increasing Fe content automatically decreases the contents of stabilizing elements (i.e. Ni and Co) which are needed to compensate the destabilizing effect of Cr. With this representation, it can also be noticed that the fcc solid solution forms a continuous domain going from pure Ni, pure fcc Co and pure fcc Fe passing by all the stable quinary compositions. Finally, thanks to this quinary section, it is now possible to choose a chemical composition which forms a solid solution and to tailor other properties such as the density, the cost or environmental considerations.

For example, the alloy $Co_5Cr_{10}Fe_{15}Mn_{60}Ni_{10}$ is predicted to form a fcc solid solution with a density of 6.814 g.cm$^{-3}$, which was calculated based on the volume and mass predicted by the Calphad method and TCHEA1 database. As a comparison, the calculated density of the quinary equimolar alloy is 7.410 g.cm$^{-3}$. Thus a decrease of 8 % of the density is achieved. One of the expected advantage of HEA is now achievable.

### *3.2. Experimental results*

In order to compare the microstructure predictions provided by the TCHEA1 database with experimental results, several alloys of the Co-Cr-Fe-Mn-Ni system were processed. Three compositions CoCrFeMn (H,H'), CrFeMnNi (B,B') and $Co_{14.5}Cr_{42}Fe_{14.5}Mn_{14.5}Ni_{14.5}$ (F,F') whose microstructure is predicted to be two-phase at 1273 and 1373 K, were prepared and annealed at 1273 K for 2 and 6 days and at 1373 K for 6 days. Four other alloys $Co_{10}Cr_{22.5}Fe_{22.5}Mn_{22.5}Ni_{22.5}$ (C), $Co_{90}Cr_{2.5}Fe_{2.5}Mn_{2.5}Ni_{2.5}$ (D), $Co_{7.5}Cr_{7.5}Fe_{7.5}Mn_{70}Ni_{7.5}$ (G) and $Co_{18.75}Cr_{25}Fe_{18.75}Mn_{18.75}Ni_{18.75}$ (E) which are predicted to be within the unique fcc solid solution domain, close from the limits, were also prepared and annealed at 1373 K for 6 days.

#### *3.2.1. Alloys predicted to be two-phase*

According to the XRD pattern (figure 3), the CoCrFeMn (H') alloy is composed of a fcc phase and a $\sigma$ phase. No qualitative microstructure evolution with duration or temperature of annealing was observed (results not shown here). Those two phases can be observed on BSE-SEM and EBSD mappings (figure 3). The fcc grain (around 10 $\mu$m) are twinned, embedded in the $\sigma$ phase. According to EDS measurements (table 2), the $\sigma$ phase is Cr-rich (32.8 at.%) whereas the fcc is slighty Cr-depleted (19.6 at.%). With a low magnification EBSD mapping, the phase volume

fractions were measured (table 2). At 1273 K, the majority phase is the $\sigma$ phase with a volume fraction of 55 %. By increasing the annealing temperature up to 1373 K, the presence of the $\sigma$ phase decreases down to 35%. On the contrary, the phase composition variation is slight.

The $Co_{14.5}Cr_{42}Fe_{14.5}Mn_{14.5}Ni_{14.5}$ (F') alloy has similar characteristics as the CoCrFeMn (H') alloy. Indeed the $Co_{14.5}Cr_{42}Fe_{14.5}Mn_{14.5}Ni_{14.5}$ (F') exhibits two phases (fcc + $\sigma$) and no microstructure evolution was noticed either with duration or temperature of annealing. According to the EBSD mapping (figure 3), the $\sigma$ phase represents more than 70 % of the volume at 1273 K. As previously, the $\sigma$ phase is Cr-rich (48.9 at.%) whereas the fcc phase is slightly Cr-depleted (27.3 at.%) compared to the nominal composition. Contrary to CoCrFeMn (H') alloy, when the annealing temperature is raised to 1373 K, the volume fraction and the phase composition of the fcc and $\sigma$ phases are stable.

The microstructure of the CrFeMnNi (B) alloy after an annealing at 1273 K for 6 days is different. Indeed, according to the XRD pattern (figure 3), this alloy is composed of three phases: fcc, bcc and $\sigma$. As can be seen on BSE-SEM and EBDS mappings, the matrix is the fcc phase in which are embedded large $\sigma$ precipitates and fine bcc needles or spheroids. The $\sigma$ and bcc phases are Cr-rich (44.2 and 56.2 at.% respectively) while the fcc phase is slightly Cr-depleted (21.1 at.%) (table 2). The fcc phase represents 85.5 % of the volume fraction while the $\sigma$ phase represents only 3.5 %. The kinetics of the phase formation of this alloy was considered. The as-cast CrFeMnNi alloy possesses only a fcc phase and the bcc phase appears after 2 days of annealing at 1273 K (results not shown here). The $\sigma$ phase was observed only after 6 days of annealing. Thus the $\sigma$ phase is stable at 1273 K but its formation is slow. After an annealing at 1373 K for 6 days, the $\sigma$ phase disappears and the alloy is two-phase (fcc + bcc) (table 2). Thus the $\sigma$ phase is not stable anymore at 1373 K.

*3.2.2. Alloys predicted to be single-phase*

The XRD pattern of the equimolar alloy CoCrFeMnNi (A') annealed at 1273 K indicates a unique fcc solid solution with a lattice parameter of 0.3603 nm (table 2). This results is confirmed by EDS-SEM analysis. For the $Co_{10}Cr_{22.5}Fe_{22.5}Mn_{22.5}Ni_{22.5}$ (C) alloy which was annealed at 1373 K, the XRD pattern indicates a single fcc phase with a lattice parameter of 0.3614 nm (table 2). The EDS-SEM analysis confirms the chemical homogeneity of the alloy. So a unique fcc solid solution is formed at 1373K. For the $Co_{18.75}Cr_{25}Fe_{18.75}Mn_{18.75}Ni_{18.75}$ (E), a unique fcc solid solution, with a lattice parameter of 0.3603 nm, is also formed at 1373 K. For $Co_{7.5}Cr_{7.5}Fe_{7.5}Mn_{70}Ni_{7.5}$ (G) alloy, the XRD pattern indicates the exclusive presence of $\beta$ Mn phase. The EDS-SEM mapping confirms the chemical homogeneity of the alloy. Finally, the XRD pattern of the $Co_{90}Cr_{2.5}Fe_{2.5}Mn_{2.5}Ni_{2.5}$ (D) which was annealed 6 days at 1373 K is indexed by the fcc and Co $\varepsilon$ phases (figure 3). EBSD mapping clearly indicates the presences of these two phases, in agreement with the XRD analysis. However no chemical variations are observed on EDS mappings. Thus the $Co_{90}Cr_{2.5}Fe_{2.5}Mn_{2.5}Ni_{2.5}$ after annealing at 1373 K for 6 days is composed of two phases with the same chemical composition but different crystallographic structure. This result will be discussed later.

## 4. Discussion

*4.1. Comparison of Calphad calculation and experimental data*

The TCHEA1 database was recently developed. Thus one aim of this study is to assess its predictive power for the Co-Cr-Fe-Mn-Ni system. To do so, 11 alloys, corresponding to 8 different compositions and 2 temperatures, were processed and characterized. With the high temperature (1273 and 1373 K) and long duration (6 days) annealings which were used, it is considered that the stable state is reached. Indeed for CoCrFeMn and $Co_{14.5}Cr_{42}Fe_{14.5}Mn_{14.5}Ni_{14.5}$ alloys annealed at 1273 K for 2 and 6 days, the microstructure does not evolve between 2 and 6 days. Furhtermore, for CrFeMnNi alloy, the $\sigma$ appears through the 6 days annealing. The annealing was long enough to from a new phase by diffusion and thus to reach the stable state.

Among the 11 alloys, 5 alloys, named A', C, D, E and G (table 2), were predicted to form a unique fcc solid solution by Calphad calculations (table 2). For three of them (i.e. alloys A', C and E), including the well-known equimolar alloy, calculations are in agreement with experimental results. For alloy D, two phases which have the same chemical composition but two distinct crystallographic structures (fcc and Co $\varepsilon$) were detected. It is well established that Co undergoes an allotropic transformation from a face centered cubic phase (fcc) to a hexagonal closed-packed phase (named $\varepsilon$) when the temperature is decreased [15]. This transformation can be compared to a martensitic transformation. It can occur at various cooling rate and it is never complete [16]. In other words, some fcc

phase always remains at room temperature. Since the fcc and Co $\varepsilon$ phases have the same chemical composition, it is very likely that the Co $\varepsilon$ phase of alloy D was formed by such a martensitic-like partial transformation of the fcc phase during the fast cooling of the sample. It means that the sample studied at room temperature is not representative of the stable state at 1373 K which was a pure fcc phase. Thus there is no contradiction between the Calphad calculations and the experimental results. Finally, alloy G, which contains 70 at.% of Mn, is composed of a unique $\beta$-Mn phase. According to the isopleth calculated with Calphad (figure 1-d), at 1373 K, for more than 80 at. % of Mn, the alloy should exhibit only a $\beta$-Mn phase. When the Mn concentration is between 75 and 80 at. %, the alloy should be two-phase and for a content of Mn lower than 75 at. %, the alloy should be composed of a unique fcc solid solution. This is not in agreement with experimental results. Thus the extent of the $\beta$-Mn domain is underestimated by at least 10 at. % and, as a consequence, the extent of the unique fcc solid solution is overestimated for high Mn concentration. In the future, other alloys will be processed to determine the exact limit of the $\beta$-Mn domain.

Alloys B, B', F, F', H and H' were predicted by Calphad to be multi-phased alloys. This is only in qualitative agreement with the experimental results. For alloys F, F', H and H', a fcc and a $\sigma$ phases were experimentally observed whereas a fcc and a bcc phases were predicted. It is mentioned that the bcc phase predicted by Calphad is Cr-rich, like experimentally observed for the $\sigma$ phase. To get more insights into this discrepancy, the evolution of phase proportions with temperature, as calculated by Calphad, are considered for the CoCrFeMn and $Co_{14.5}Cr_{42}Fe_{14.5}Mn_{14.5}Ni_{14.5}$ compositions (figure 4). Bcc and fcc phases are predicted to be first formed after solidification and the $\sigma$ phase should appear at 1040 and 814 K for CoCrFeMn and $Co_{14.5}Cr_{42}Fe_{14.5}Mn_{14.5}Ni_{14.5}$, respectively. Thus the temperature range of stability of the $\sigma$ phase and bcc phase are respectively underestimated and overestimated by Calphad calculations. Similarly, for alloy B, at 1273 K, fcc, bcc and $\sigma$ phases were observed whereas Calphad method predicted only the presence of fcc and bcc phases. More precisely, the $\sigma$ phase is calculated to be stable for this composition for temperatures below 1060 K (figure 4). For alloy B, which was annealed at 1373 K, no $\sigma$ phase was observed, in agreement with calculations. Thus, once again, Calphad calculations underestimate the temperature range of existence of the $\sigma$ phase. It should be underlined that the calculated compositions of the fcc phases of alloys B, B', F, F', H and H' are in very good agreement with the experimental measurements. The composition of the fcc phases of multi-phased alloys correspond to boundaries of the existence domain of the fcc solid solution. This is well calculated by Calphad.

To further assess the validity of the TCHEA1 database, the Calphad calculations on the Co-Cr-Fe-Mn-Ni system are now compared to experimental data from the literature. First, concerning the quinary equimolar CoCrFeMnNi alloy, it has been widely established, including in this study, that its stable state at high temperature is a unique fcc solid solution [6, 1, 17]. However, Otto et al.[18] recently studied this alloy at lower temperatures with extremely long annealing time. The objective was to reach the thermodynamical equilibrium, despite the very slow diffusion [19]. It was observed that the alloy is still a unique fcc solid solution at 1173 K. However, at 973 K, a Cr-rich $\sigma$ phase precipitates and, at 773 K, several phases, including a Cr-rich bcc phase, are formed. For the equimolar CoCrFeMnNi alloy, the appearance of the $\sigma$ phase and of the bcc is predicted at 873 and 773 K by Calphad calculations (figure 4), which is in good agreement with experimental data, although the temperature range of existence of the $\sigma$ phase is one more time slightly underestimated. Several non-equimolar compositions have also been studied experimentally. The following compositions have been selected to be compared to our Calphad calculations: $Co_{10}Cr_{10}Fe_{40}Mn_{40}$ [10], $Co_5Cr_2Fe_{40}Mn_{27}Ni_{26}$ [9], $Co_{(5.6)}Cr_{(2.3)}Fe_{(64-x)}Mn_xNi_{(27.7)}$ with x = 21, 24, 27, 34 and 38 (at. %) [20], $Cr_xFe_{40}Mn_{28}Ni_{(32-x)}$ with x = 4, 12, 18 and 24 (at.%) [21]. All these alloys were homogeneized at temperatures between 1273 and 1473 K for durations long enough to be considered as representative of the stable state. Moreover they were characterized by XRD, EDS-SEM and for some of them [9, 10] by atom probe tomography, which guarantees a reliable phase identification. For the $Cr_{24}Fe_{40}Mn_{28}Ni_8$ [21], fcc and $\sigma$ phases were observed whereas Calphad calculations predict fcc and bcc phases. Once again, the stability of the $\sigma$ phase is underestimated by the Calphad calculations. The other 10 alloys were both observed and calculated as being a unique fcc solid solution.

In order to find a reason for the underestimation of the $\sigma$ phase by the TCHEA1 database, the 10 ternary constituting systems were investigated. The 5 ternary systems optimized in the TCHEA1 database have good agreement with experimental phase diagrams. The 5 ternary systems which were not optimized on experimental data (i.e. which were only extrapolated from binary systems) are considered. The Co-Fe-Mn diagram is in good agreement with experimental data. For Co-Cr-Mn and Co-Mn-Ni, no experimental data exists. For Cr-Mn-Ni, discrepancies appear between calculated and experimental diagrams. However, the experimental composition range of the $\sigma$ phase domain is not extended at high temperature. Finally, there are also discrepancies for Cr-Fe-Mn, which seem to be more significant.

Indeed, in the 1073 K experimental diagram [22], the $\sigma$ phase domain is extended and continuous from Cr-Mn to Cr-Fe. On the contrary, it is discontinuous in the calculated diagram (see Supplementary Material 3a). Moreover, at 1473 K, $\sigma$ phase domains of the calculated and experimental diagrams are not overlapping (see Supplementary Material 3b) [22]. The phase diagram of the binary Cr-Mn system is described using two $\sigma$ phases. The usual one is the phase at low temperature (it is the same $\sigma$ phase as in Fe-Cr and Co-Cr system and it accepts solubility of all elements), while the high temperature form is only a binary phase (it has no solubility of any other element). This is the reason why it does not appear in the 1473 K isothermal section. A second consequence may be an underestimation of the stability of the $\sigma$ phase having consequences not only in the ternary but also in the quinary Co-Cr-Fe-Mn-Ni system. As a matter of fact, the 4 previously mentioned alloys for which the $\sigma$ phase was not predicted (i.e. CrFeMnNi, CoCrFeMn, $Co_{14.5}Cr_{42}Fe_{14.5}Mn_{14.5}Ni_{14.5}$ and $Cr_{24}Fe_{40}Mn_{28}Ni_8$) are all concentrated in Cr, Fe and Mn. We suggest that the ternary Cr-Fe-Mn system and perhaps also the binary Cr-Mn system should be reassessed. We can also not exclude that other errors may originate from a poor description of Co-Cr-Mn and Cr-Mn-Ni systems.

To conclude, the Calphad method and the TCHEA1 database very reliably describe the existence domain of the fcc solid solution. Indeed 14 compositions, i.e. 4 within this study and 10 from the literature, were both experimentally and by calculations shown to form a unique fcc solid solution. Moreover, the boundaries of the fcc existence domain as predicted by Calphad were experimentally confirmed for 6 compositions of fcc phases, from multi-phased alloys processed in this study. There is a disagreement for only one composition, which was predicted by Calphad to form a fcc solid solution and which was experimentally proven to form another phase. Since this alloy was close to a boundary of the fcc domain according to Calphad, this disagreement does not question the whole reliability of the TCHEA1 database. Concerning multi-phased alloys, it was shown for 5 alloys that the Calphad method based on the TCHEA1 database does not predict the correct phases. More precisely, the stability of the $\sigma$ phase is largely underestimated.

### *4.2. Thermodynamic behavior of HEA*

At first, multi-component and very concentrated solid solutions were thought to be stabilized by a high configurational entropy [2] and that is why the name "high entropy alloys" emerged. Since then, the non-predominant role of configurational entropy has been exposed several times [11, 6, 5]. This study reinforces this statement. Indeed, it was shown for several alloys that the unique fcc solid solution demixes into fcc, $\sigma$ and/or bcc phases. Since these phases are disordered or partially ordered, they are also stabilized by configurational entropy. In other words, Thus, one more time, it should be emphasized that, as for any materials, the phase stability in HEA is determined by the Gibbs energy and not only by the entropy.

Later on, based on the Hume-Rothery rules, it was proposed to consider the crystal structure, size and electronegativity of pure metals in order to choose appropriate elements to form a unique solid solution [23]. Those criteria were rejected for being non predictive [5]. Still, for the Co-Cr-Fe-Mn-Ni system, for which it was already known that the equimolar composition can form a single solid solution, those Hume-Rothery based rules can qualitatively explain the influence of each element on the solid solution stability. Indeed, the most destabilizing element was shown to be Cr. This is also the only element of the system which does not form a stable fcc phase, at any temperature [24]. The second destabilizing element is Mn, which has the largest atomic size [24].

An empirical criterion based on the valence electron concentration (VEC) was also proposed to predict the phase formation in HEA [25]. Recently, Tsai *et al.* has shown that the VEC criterion alone could not predict the $\sigma$ phase formation [26]. Since the $\sigma$ phase reduces the tensile ductility of HEA [27], predicting its formation is essential. Thus Tsai *et al.* proposed to combine the VEC criterion with a second criterion based on alloy composition [26]. This approach is in agreement with the experimental results of this study (i.e.: the $\sigma$ phase is formed for the 3 alloys respecting those two criteria). However, in this approach, the influence of temperature on phase stability is not taken into account and thus the predictions cannot be complete. For example, the fact that for CrFeMnNi alloy (B and B'), the $\sigma$ phase is present at 1273 K and then disappears at 1373 K cannot be predicted. Still, prior to produce an alloy and waiting for a better description of the $\sigma$ phase by the TCHEA1 database, calculating the VEC and alloy composition criteria as exposed in [26] is of interest.

Finally, this study fully illustrates that the solid solution stability is well described by the Calphad method and, as a consequence, that the Calphad method is appropriate to study phase stability of HEA. Thus thermodynamic laws, which have been used for years to describe binary and ternary alloys [28], can also be applied to multi-component alloys. More broadly, the Calphad method will be useful for the design and development of multi-component alloys,

not only to find appropriate composition for single-phased alloys but also to strengthen alloys through precipitation hardening. It has to be underlined that, to do so, a significant improvement of the TCHEA1 database and thus additional experimental work are required. The results obtained in this study could contribute to improve the TCHEA1 database.

## 5. Summary and conclusions

The phase stability of the fcc solid solution within the Co-Cr-Fe-Mn-Ni system was theoretically and experimentally studied. Using the Calphad method and the new TCHEA1 database, 5 isopleths were plotted and the stable phases of 10 626 compositions were determined. Moreover, 11 alloys were processed and characterized. The main results are the following:

- The existence domain of the fcc solid solution is very accurately described by the TCHEA1 database. On the contrary, the $\sigma$ phase stability is underestimated by this database, resulting in an incorrect description of multi-phased alloys,
- The existence domain of the fcc solid solution for the Co-Cr-Fe-Mn-Ni was completely described at 1273 K. This domain is very extended. Now it is possible to choose a chemical composition which forms a solid solution and to optimize other properties,
- Increasing Cr or, in a lesser extent, Mn contents destabilizes the fcc solid solution. When combined, this destabilizing effect is amplified. On the contrary, Ni and Co stabilize the fcc solution.

In the future, the evolution of the fcc solid solution strengthening with composition will be explored.

## 6. Acknowledgments

The author is grateful to J.-P Couzinié for fruitful discussions. The technical help from Y. Cotrebil and V. Lalanne is greatly appreciated. This work has benefited from a French government grant managed by ANR within the frame of the national program Investments for the Future ANR-11-LABX-022-01.

## References

[1] B. Cantor, I. Chang, P. Knight, A. Vincent, Microstructural development in equiatomic multicomponent alloys, Materials Science and Engineering: A 375-377 (2004) 213–218. doi:10.1016/j.msea.2003.10.257.

[2] J.-W. Yeh, S.-K. Chen, S.-J. Lin, J.-Y. Gan, T.-S. Chin, T.-T. Shun, C.-H. Tsau, S.-Y. Chang, Nanostructured high-entropy alloys with multiple principal elements: Novel alloy design concepts and outcomes, Advanced Engineering Materials 6 (5) (2004) 299–303. doi:10.1002/adem.200300567.

[3] Y. Zhang, T. T. Zuo, Z. Tang, M. C. Gao, K. A. Dahmen, P. K. Liaw, Z. P. Lu, Microstructures and properties of high-entropy alloys, Progress in Materials Science 61 (2014) 1–93. doi:10.1016/j.pmatsci.2013.10.001.

[4] J.-W. Yeh, Alloy design strategies and future trends in high-entropy alloys 65 (12) (2013) 1759–1771. doi:10.1007/s11837-013-0761-6.

[5] F. Otto, Y. Yang, H. Bei, E. George, Relative effects of enthalpy and entropy on the phase stability of equiatomic high-entropy alloys, Acta Materialia 61 (7) (2013) 2628–2638. doi:10.1016/j.actamat.2013.01.042.

[6] M. Laurent-Brocq, L. Perrière, R. Pirès, Y. Champion, From high entropy alloys to diluted multi-component alloys: Range of existence of a solid-solution, Materials & Design 103 (2016) 84–89. doi:10.1016/j.matdes.2016.04.046.

[7] S. Guo, Phase selection rules for cast high entropy alloys: an overview, Materials Science and Technology 31 (10) (2015) 1223–1230. doi:10.1179/1743284715Y.0000000018.

[8] M. C. Troparevsky, J. R. R. K. Morris, A. R. Lupini, G. M. Stocks, Criteria for predicting the formation of single-phase high-entropy alloys, Physical Review X 5 (1). doi:10.1103/PhysRevX.5.011041.

[9] M. Yao, K. Pradeep, C. Tasan, D. Raabe, A novel, single phase, non-equiatomic FeMnNiCoCr high-entropy alloy with exceptional phase stability and tensile ductility, Scripta Materialia 72-73 (2014) 5–8. doi:10.1016/j.scriptamat.2013.09.030.

[10] Y. Deng, C. Tasan, K. Pradeep, H. Springer, A. Kostka, D. Raabe, Design of a twinning-induced plasticity high entropy alloy, Acta Materialia 94 (2015) 124–133. doi:10.1016/j.actamat.2015.04.014.

[11] D. Ma, M. Yao, K. Pradeep, C. C. Tasan, H. Springer, D. Raabe, Phase stability of non-equiatomic CoCrFeMnNi high entropy alloys, Acta Materialia 98 (2015) 288–296. doi:10.1016/j.actamat.2015.07.030.

[12] O. Senkov, J. Miller, D. Miracle, C. Woodward, Accelerated exploration of multi-principal element alloys with solid solution phases, Nature Communications 6 (2015) 6529. doi:10.1038/ncomms7529.
[13] Thermo-Calc Software, Thermodynamic databases, http://www.thermocalc.com/products-services/databases/thermodynamic/, accessed: 2016-12-28.
[14] J. Rodríguez-Carvajal, Fullprof: a program for rietveld refinement and pattern matching analysis, in: satellite meeting on powder diffraction of the XV congress of the IUCr, Toulouse, France, Vol. 127, 1990, p. 13.
[15] T. Nishizawa, K. Ishida, The cofe (cobaltiron) system, Bulletin of Alloy Phase Diagrams 5 (3) (1984) 250. doi:10.1007/BF02868548.
[16] Z. Nishiyama, Martensitic transformation, Elsevier, 2012.
[17] Z. Wu, H. Bei, F. Otto, G. Pharr, E. George, Recovery, recrystallization, grain growth and phase stability of a family of FCC-structured multi-component equiatomic solid solution alloys, Intermetallics 46 (2014) 131–140. doi:10.1016/j.intermet.2013.10.024.
[18] F. Otto, A. Dlouh, K. Pradeep, M. Kubnov, D. Raabe, G. Eggeler, E. George, Decomposition of the single-phase high-entropy alloy CrMnFeCoNi after prolonged anneals at intermediate temperatures, Acta Materialia 112 (2016) 40–52. doi:10.1016/j.actamat.2016.04.005.
[19] K.-Y. Tsai, M.-H. Tsai, J.-W. Yeh, Sluggish diffusion in cocrfemnni high-entropy alloys, Acta Materialia 61 (13) (2013) 4887–4897. doi:10.1016/j.actamat.2013.04.058.
[20] K. Pradeep, C. Tasan, M. Yao, Y. Deng, H. Springer, D. Raabe, Non-equiatomic high entropy alloys: Approach towards rapid alloy screening and property-oriented design, Materials Science and Engineering: A 648 183–192. doi:10.1016/j.msea.2015.09.010.
[21] N. Stepanov, D. Shaysultanov, M. Tikhonovsky, G. Salishchev, Tensile properties of the crfenimn non-equiatomic multicomponent alloys with different cr contents, Materials & Design 87 (2015) 60–65. doi:10.1016/j.matdes.2015.08.007.
[22] G. V. Raynor, V. G. Rivlin, Phase equilibria in iron ternary alloys–a critical assessment of the experimental literature, The Institute of Metals, 1 Carlton House Terrace (1988) 288–299.
[23] Y. Zhang, Y. Zhou, J. Lin, G. Chen, P. Liaw, Solid-solution phase formation rules for multi-component alloys, Advanced Engineering Materials 10 (6) (2008) 534–538. doi:10.1002/adem.200700240.
[24] W. B. Pearson, A handbook of lattice spacings and structures of metals and alloys, 1967.
[25] S. Guo, C. Ng, J. Lu, C. T. Liu, Effect of valence electron concentration on stability of fcc or bcc phase in high entropy alloys, Journal of Applied Physics 109 (10) (2011) 103505. doi:10.1063/1.3587228.
[26] M.-H. Tsai, K.-C. Chang, J.-H. Li, R.-C. Tsai, A.-H. Cheng, A second criterion for sigma phase formation in high-entropy alloys, Materials Research Letters 4 (2) (2016) 90–95. doi:10.1080/21663831.2015.1121168.
[27] N. Stepanov, D. Shaysultanov, G. Salishchev, M. Tikhonovsky, E. Oleynik, A. Tortika, O. Senkov, Effect of v content on microstructure and mechanical properties of the CoCrFeMnNiVx high entropy alloys, Journal of Alloys and Compounds 628 (2015) 170–185. doi:10.1016/j.jallcom.2014.12.157.
[28] H. L. Lukas, S. G. Fries, B. Sundman, Computational thermodynamics: the Calphad method, Vol. 131, Cambridge university press Cambridge, 2007.

## Captions

**Figure 1 :** Isopleth sections calculated with the Calphad method and the TCHEA1 database for a) Co-CrFeMnNi, b) Cr-CoFeMnNi, c) Fe-CoCrMnNi, d) Mn-CoCrFeNi and e) Ni-CoCrFeMn. The black dashed line and the red/blue circles represent the equimolar composition and the processed alloys of this study predicted to be two-phase/single-phase, respectively. The domain of existence of the single fcc phase is dashed with blue lines.

**Figure 2 :** Quinary section of the Co-Cr-Fe-Mn-Ni system at 1273 K which represents the stable phases of the 10626 compositions calculated with the Calphad method and the TCHEA1 database. One quasi-ternary phase diagram is zoomed within the black rectangle. A blue square indicates a unique fcc solid solution whereas a red square indicates other cases (several phases, bcc phase ...). The absence of a square means that the composition does not exist. Quasi-ternary diagrams are not plotted (i.e. for high Mn or Cr contents) when they include no unique fcc solid solution.

**Figure 3 :** Characterization of alloys H', F', B' (predicted to be two-phase) and D (predicted to be single-phase). (Left) X-ray diffraction patterns. (Middle) BSE-SEM images and (Right) EBSD mappings.

**Figure 4 :** Evolution with temperature of the phase amount calculated with the Calphad method and the TCHEA1 database for CoCrFeMnNi, CoCrFeMn, CrFeMnNi and $Co_{14.5}Cr_{42}Fe_{14.5}Mn_{14.5}Ni_{14.5}$. The grey dashed line represent the processed alloys.

**Table 1 :** Percentage of $Co_vCr_wFe_xMn_yNi_z$ compositions forming a unique fcc solid solution as calculated with the Calphad method for various number of elements (n) and at two temperatures.

**Table 2 :** Experimental and calculated data for all processed alloys which were annealed at 1273 or 1373 K for 6 days. For the experimental data, the volume fraction, composition and lattice parameter were measured by EBSD, EDS-SEM and XRD, respectively. The standard deviations refer to the last digit and are indicated between brackets. Calculation was done with the Calphad method and the TCHEA1 database.

**Supplementary Material 1 :** Fe-Mn phase diagram calculated with the Calphad method and based on a) TCFE7 b) TCHEA1 database.

**Supplementary Material 2 :** Quinary section of the Co-Cr-Fe-Mn-Ni system at 1273 K which represents the stable phases of the 10626 compositions calculated with the Calphad method and the TCHEA1 database. One quasi-ternary phase diagram is zoomed within the black rectangle. A blue square indicates a unique fcc solid solution whereas a red square indicates other cases (several phases, bcc phase ...). The absence of a square means that the composition does not exist. Quasi-ternary diagrams are not plotted (i.e. for high Ni or Co contents) when they include only unique fcc solid solution.

**Supplementary Material 3 :** Isothermal section of the Cr-Fe-Mn phase diagram calculated with the Calphad method and based on the TCHEA1 database at a) 1073 K b) 1473 K. Experimental $\sigma$ phase domain comes from [22].

Figure 1

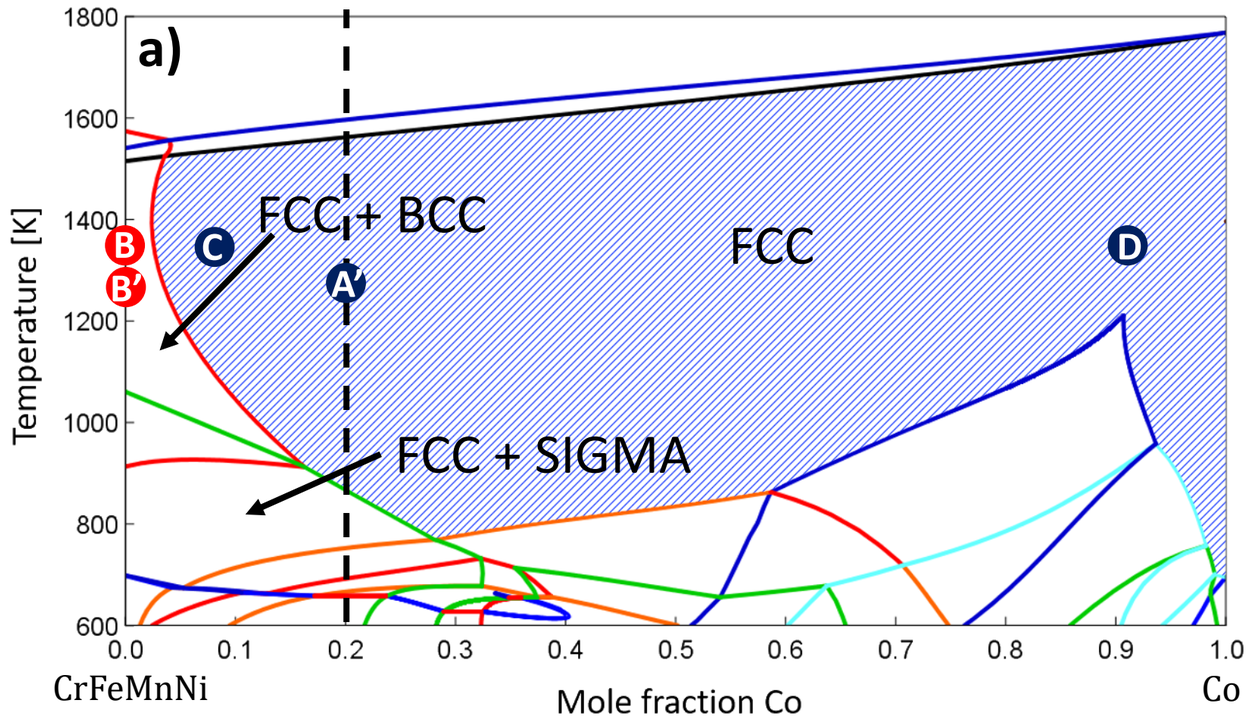
a)
FCC + BCC
FCC
FCC + SIGMA
A′
B
B′
C
D
Temperature [K]
CrFeMnNi
Mole fraction Co
Co

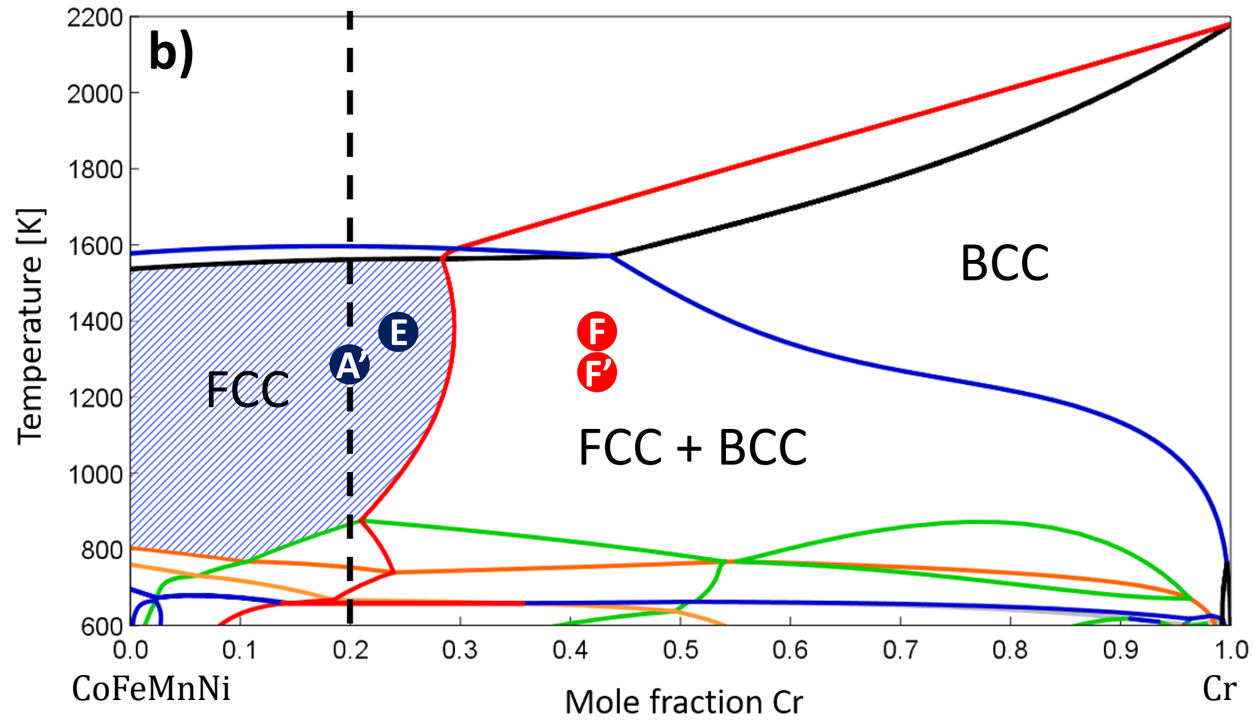
b)
BCC
FCC
FCC + BCC
A′
E
F
F′
Temperature [K]
CoFeMnNi
Mole fraction Cr
Cr

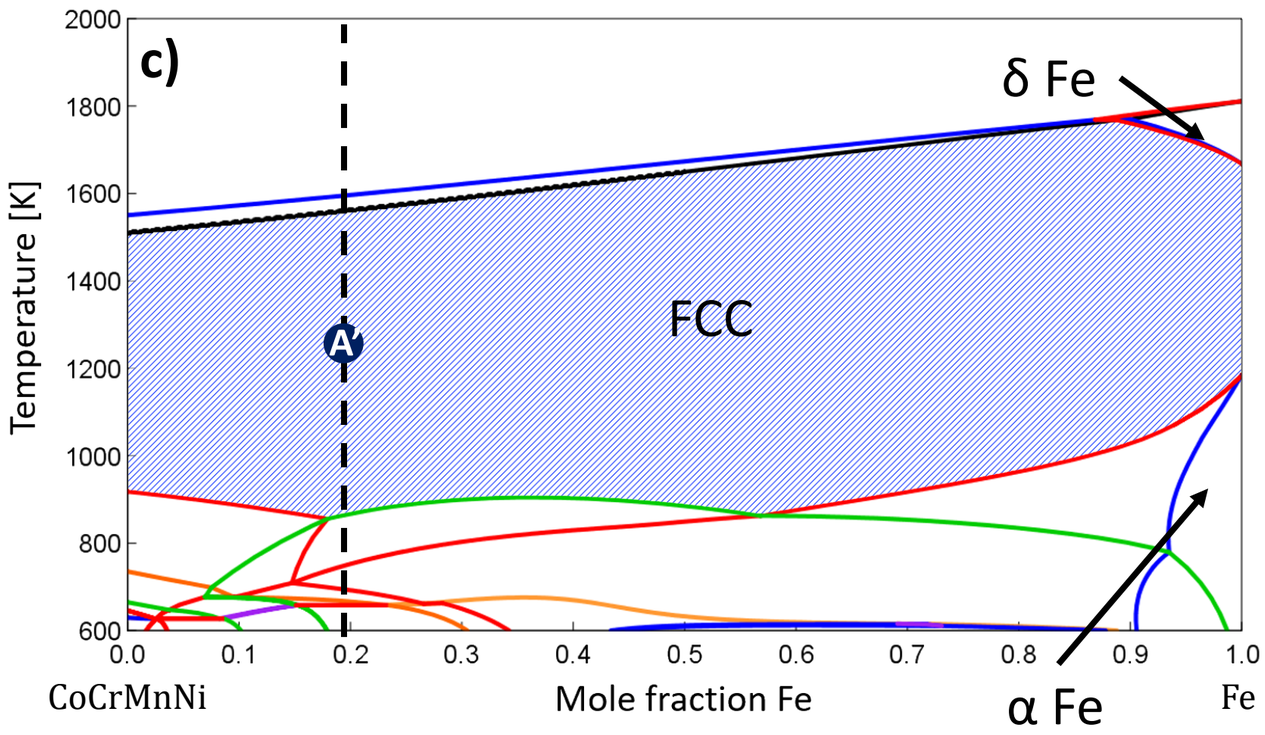
c)
δ Fe
FCC
A′
Temperature [K]
CoCrMnNi
Mole fraction Fe
α Fe
Fe

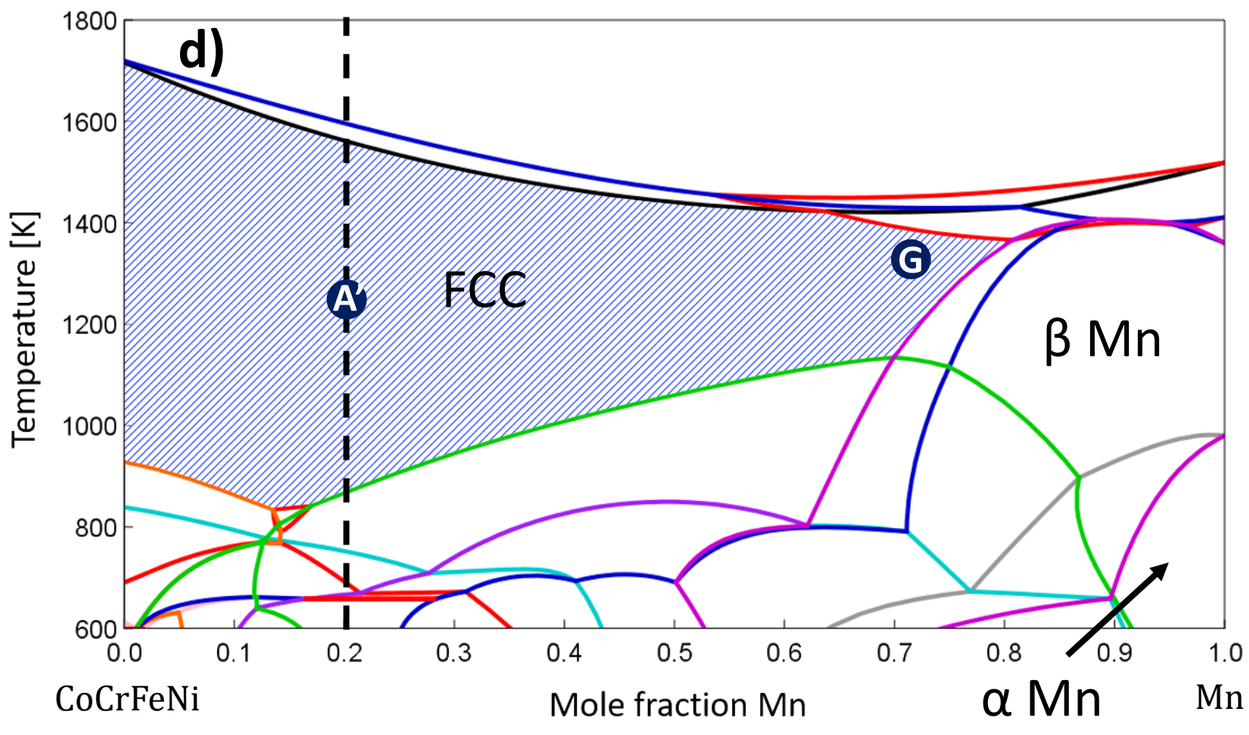
d)
FCC
A′
G
β Mn
α Mn
Temperature [K]
CoCrFeNi
Mole fraction Mn
Mn

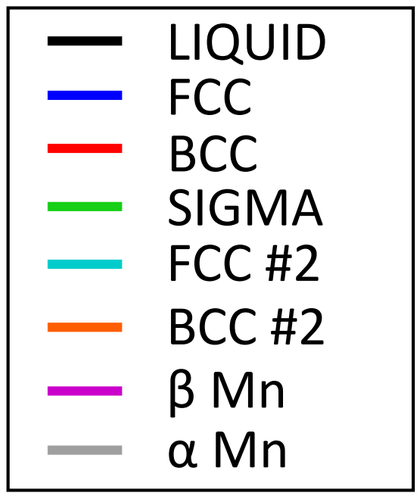
LIQUID
FCC
BCC
SIGMA
FCC #2
BCC #2
β Mn
α Mn

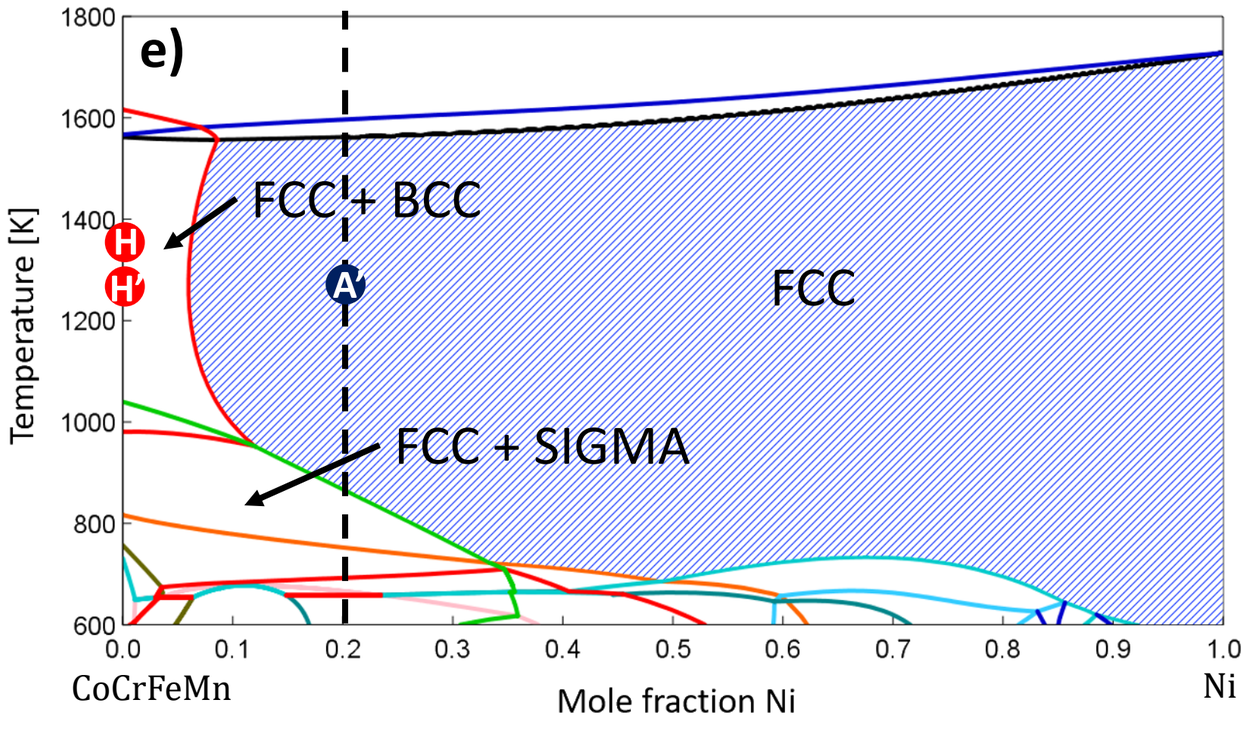
e)
FCC + BCC
FCC
FCC + SIGMA
A′
H
H′
Temperature [K]
CoCrFeMn
Mole fraction Ni
Ni

Figure2

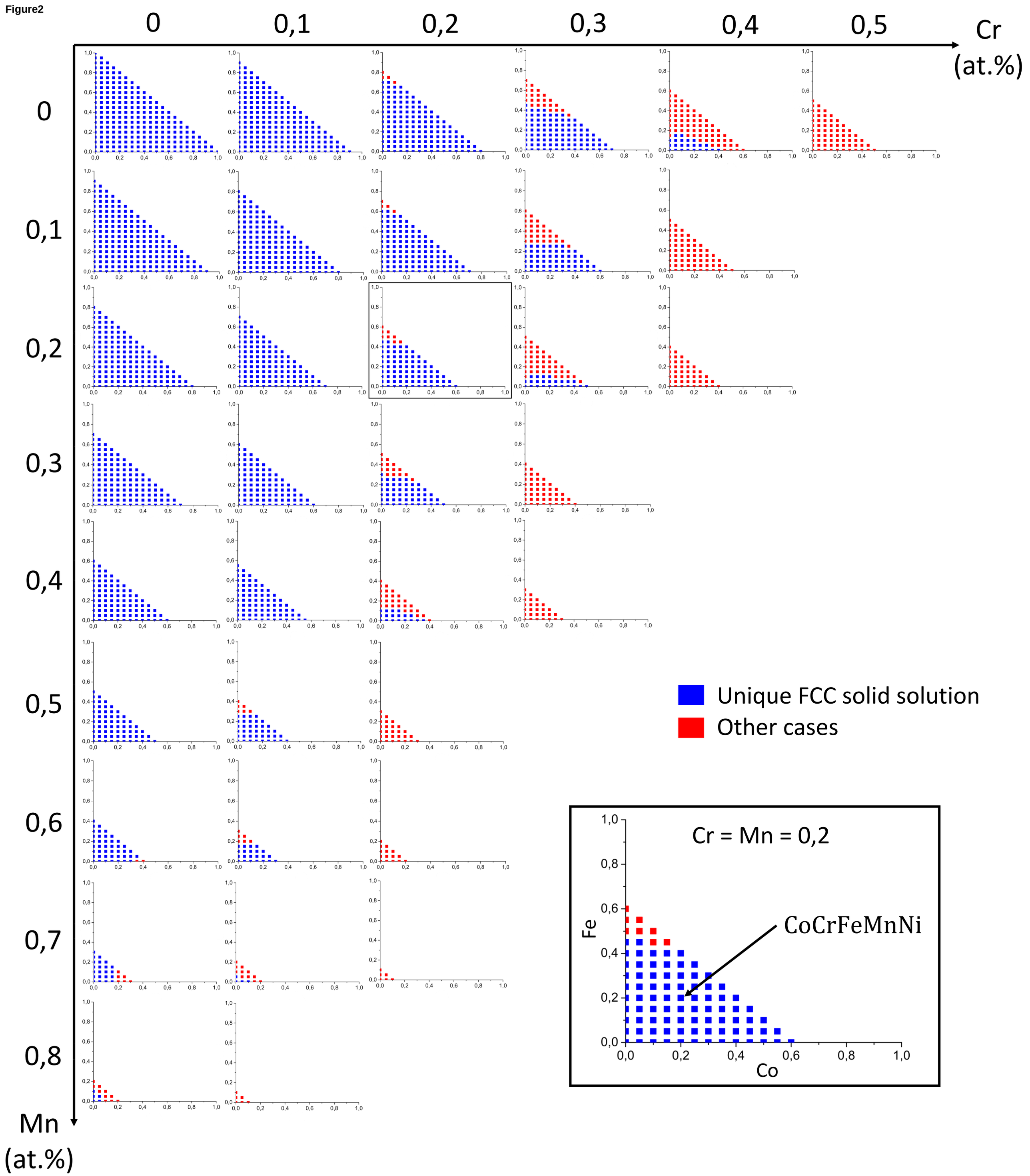
0
0,1
0,2
0,3
0,4
0,5
0,6
0,7
0,8
Cr (at.%)
Mn (at.%)
Unique FCC solid solution
Other cases
Cr = Mn = 0,2
CoCrFeMnNi
Fe
Co

Figure3

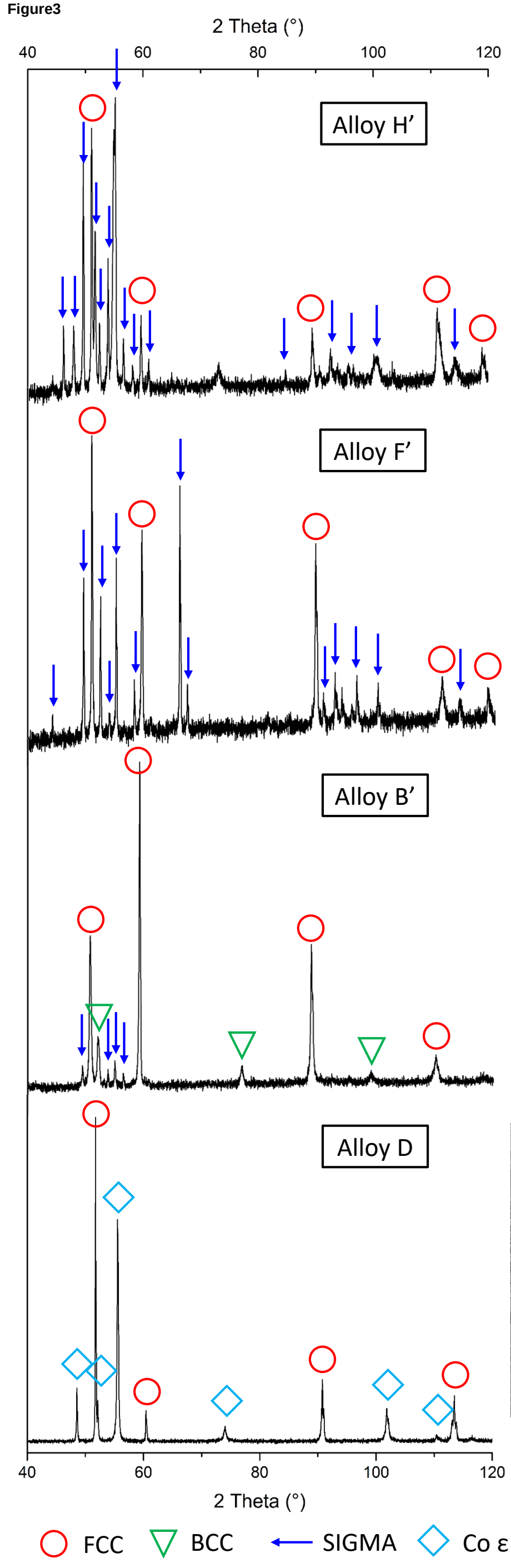


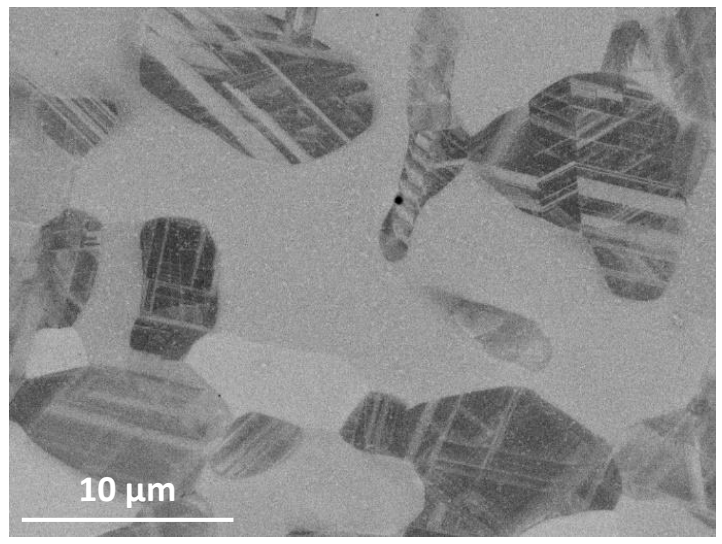


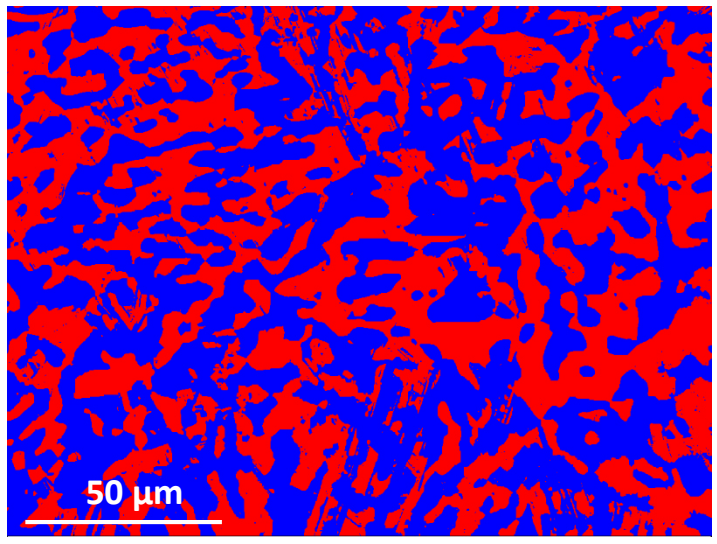


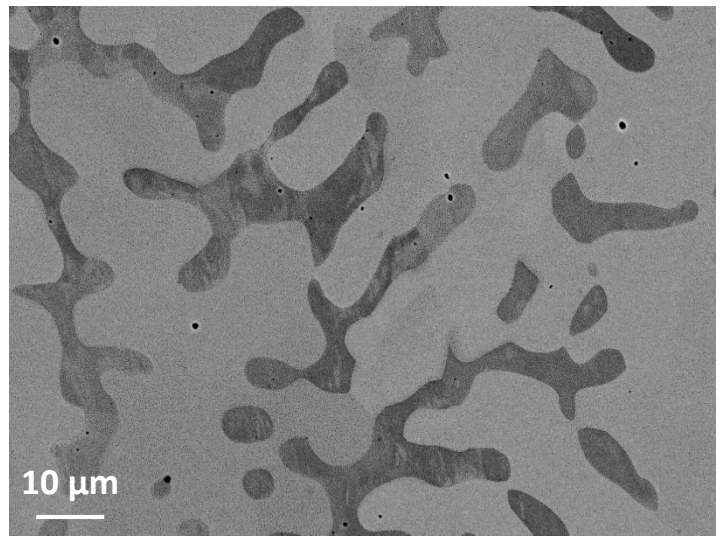


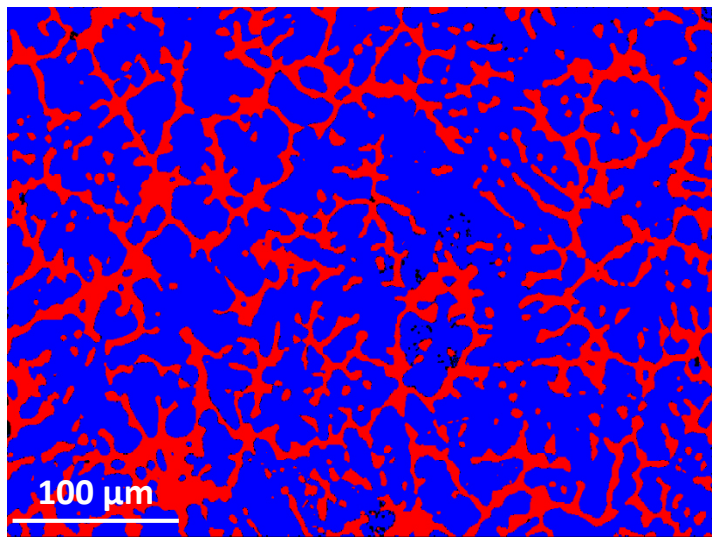


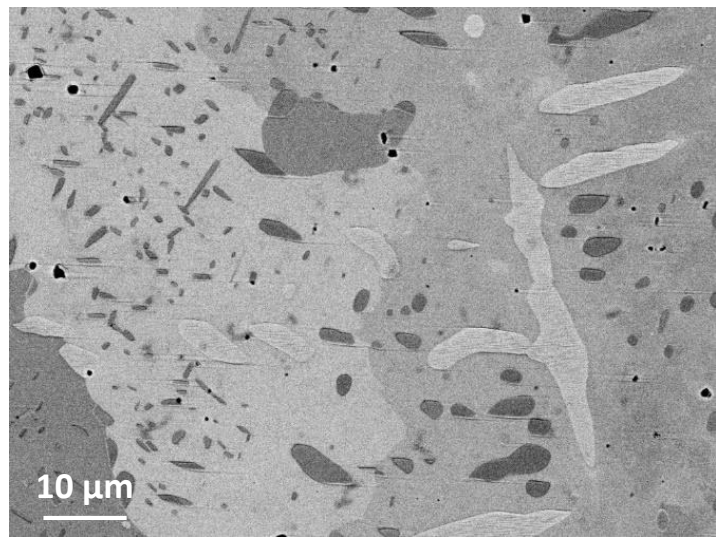


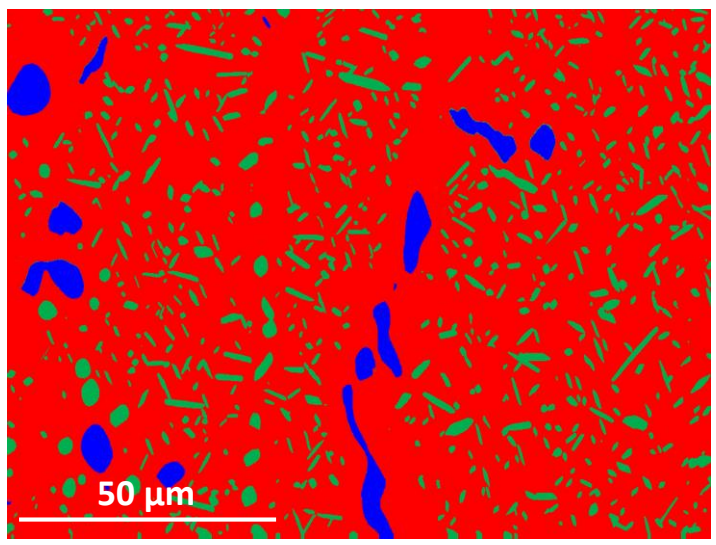


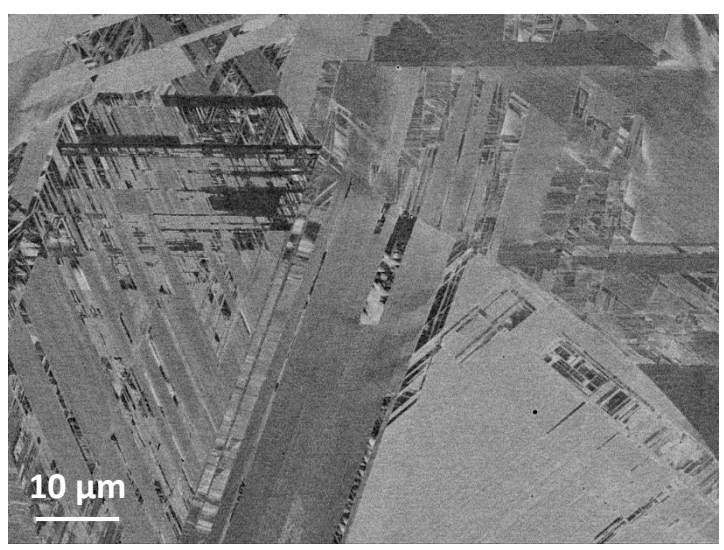


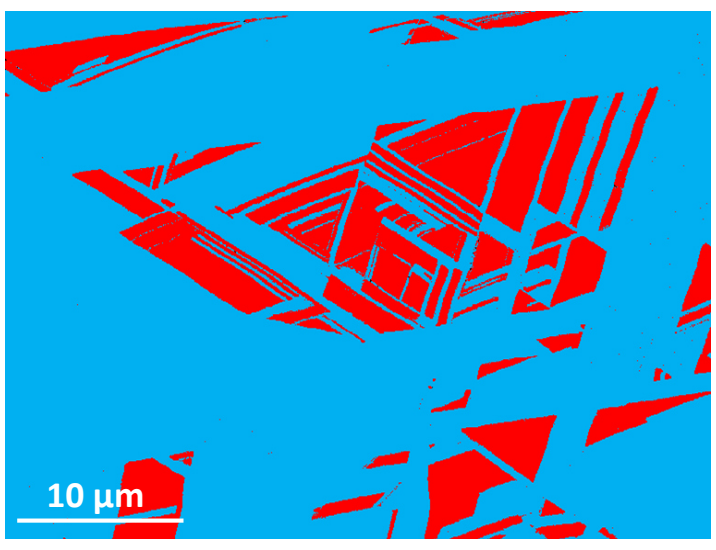


FCC SIGMA
BCC Co ε

**Figure4**

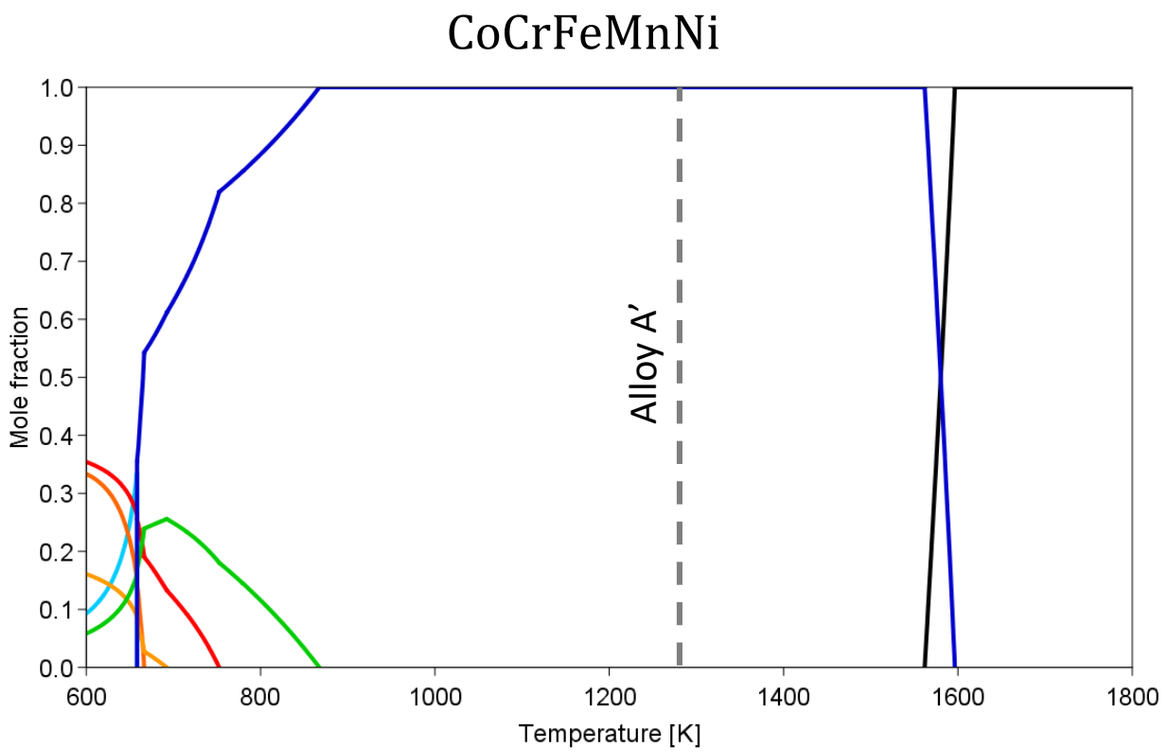
CoCrFeMnNi
Mole fraction
Temperature [K]
Alloy A’

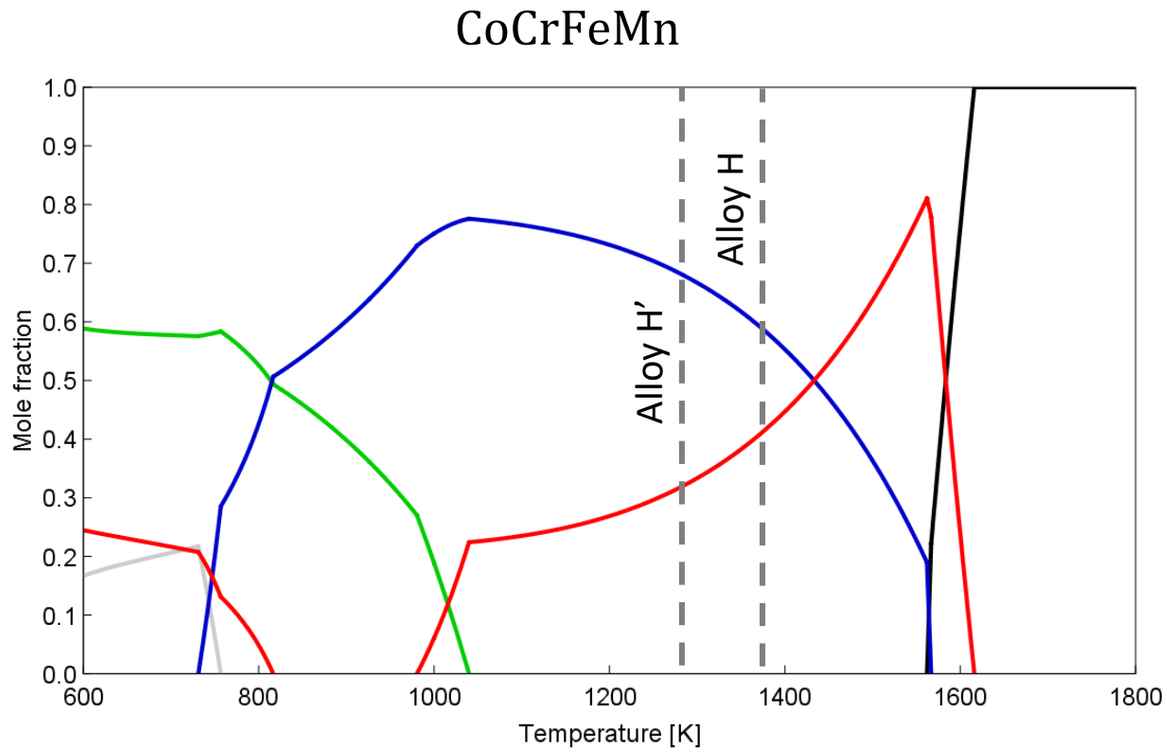
CoCrFeMn
Mole fraction
Temperature [K]
Alloy H’
Alloy H

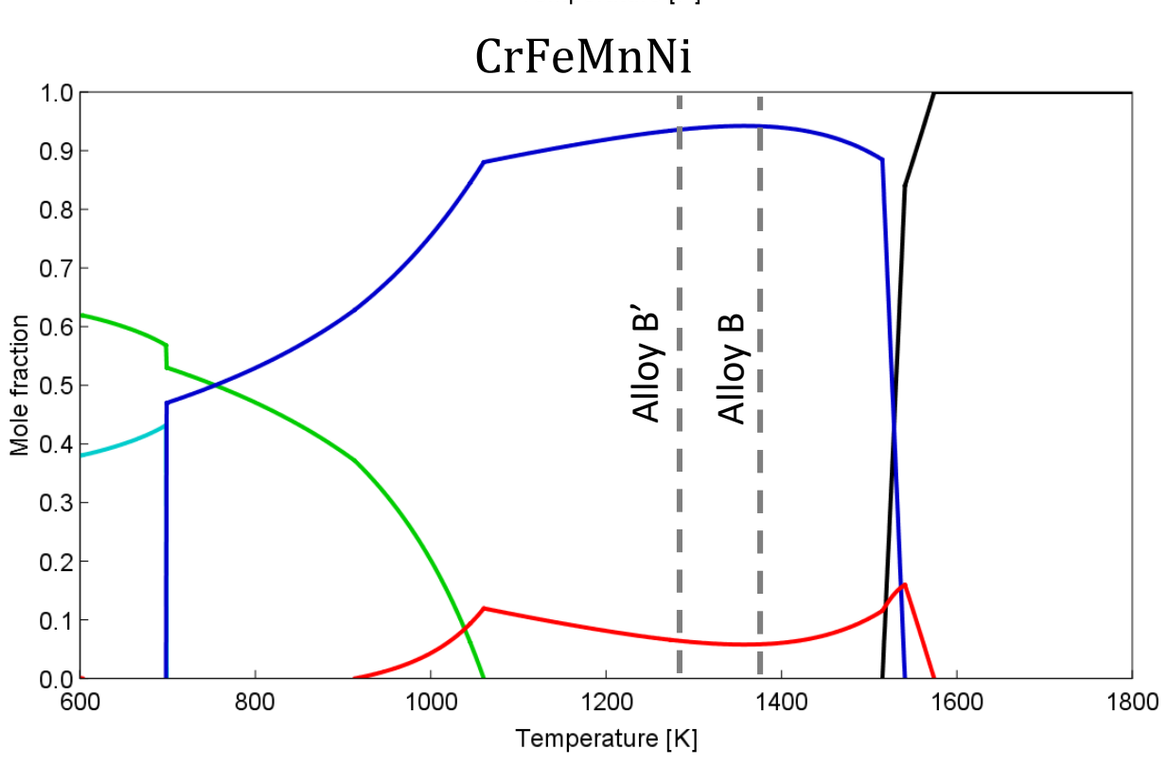
CrFeMnNi
Mole fraction
Temperature [K]
Alloy B’
Alloy B

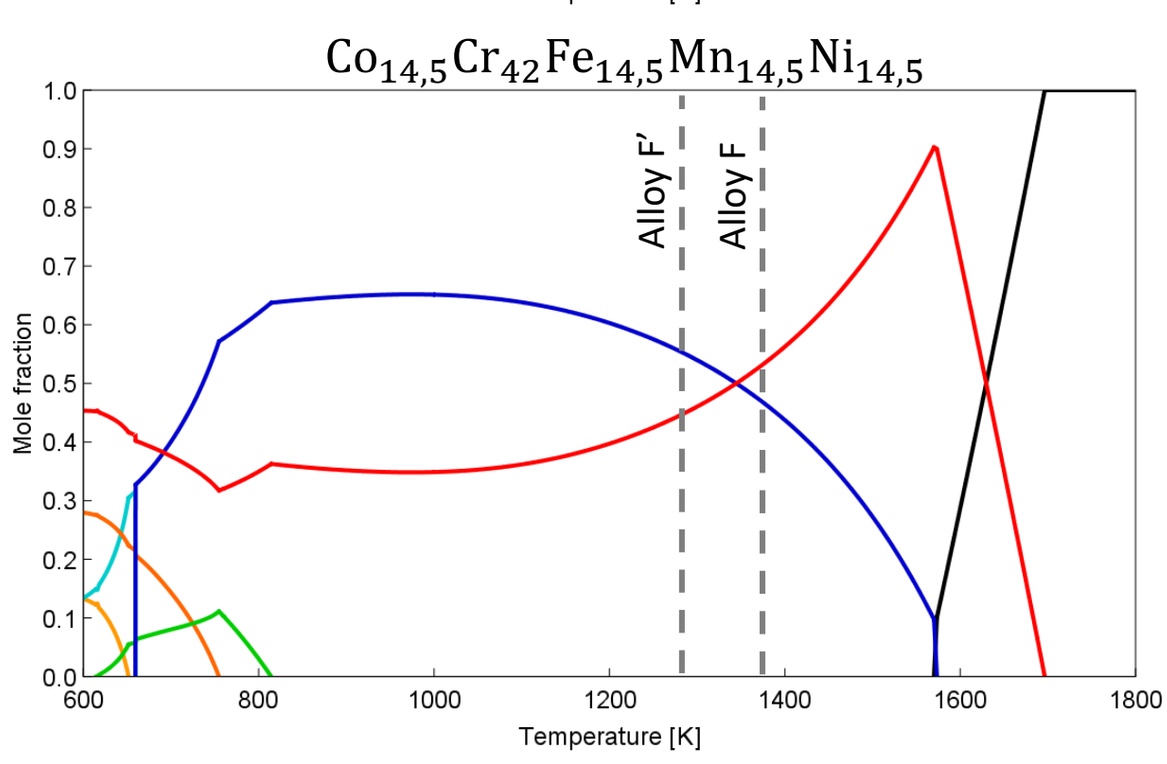
$Co_{14,5}Cr_{42}Fe_{14,5}Mn_{14,5}Ni_{14,5}$
Mole fraction
Temperature [K]
Alloy F’
Alloy F


LIQUID
FCC
BCC
SIGMA
BCC #2
FCC #2
HCP

**Table1**

| n | 1273 K | 1373 K |
|---|---|---|
| 2 | 45.8 % | 42.1 % |
| 3 | 65.1 % | 63.9 % |
| 4 | 67.0 % | 66.8 % |
| 5 | 73.1 % | 73.3 % |
| Total | 68.5 % | 68.2 % |

Table 2

| Sample | Annealing temperature (K) | Nominal composition (at.%) | | | | | Experimental | | | | | | | Calculated | | | | | | |
|---|---|---|---|---|---|---|---|---|---|---|---|---|---|---|---|---|---|---|---|---|
| | | | | | | | Phase | Volume fraction | Composition (at.%) | | | | | Phase | Volume fraction | Composition (at.%) | | | | |
| | | Co | Cr | Fe | Mn | Ni | | | Co | Cr | Fe | Mn | Ni | | | Co | Cr | Fe | Mn | Ni |
| A' | 1273 | 20 | 20 | 20 | 20 | 20 | FCC | 100.0 | 20.0 | 20.3 | 20.0 | 20.3 | 19.4 | $a$=0.3603(2) | FCC | 100.0 | 20.0 | 20.0 | 20.0 | 20.0 | 20.0 |
| B | 1373 | - | 25 | 25 | 25 | 25 | FCC | 93.8 | - | 23.8(1) | 24.9(1) | 25.8(1) | 25.5(1) | $a$=0.3622(2) | FCC | 94.2 | - | 23.8 | 25.1 | 25.3 | 25.8 |
| | | | | | | | BCC | 6.2 | - | 46.6(6) | 24.8(3) | 17.9(3) | 10.7(5) | $a$=0.2889(1) | BCC | 5.8 | - | 43.6 | 23.2 | 20.8 | 12.4 |
| B' | 1273 | - | 25 | 25 | 25 | 25 | FCC | 85.5 | - | 21.1(1) | 25.1(1) | 26.7(2) | 27.1(2) | $a$=0.3619(2) | FCC | 93.4 | - | 23.3 | 25.2 | 25.4 | 26.1 |
| | | | | | | | BCC | 11.0 | - | 56.2(7) | 22.4(3) | 14.8(2) | 6.6(3) | $a$=0.2881(1) | BCC | 6.6 | - | 49.0 | 22.1 | 19.6 | 9.3 |
| | | | | | | | $\sigma$ | 3.5 | - | 44.2(3) | 25.7(1) | 18.7(1) | 11.4(2) | $a$=0.8826(1) $c$=0.4570(2) | | | | | | | |
| C | 1373 | **10** | 22.5 | 22.5 | 22.5 | 22.5 | FCC | 100.0 | 10.0 | 23.1 | 22.5 | 22.5 | 22.5 | a=0.3614(1) | FCC | 100.0 | 10.0 | 22.5 | 22.5 | 22.5 | 22.5 |
| D | 1373 | **90** | 2.5 | 2.5 | 2.5 | 2.5 | FCC | 22.7 | 88.1 | 2.6 | 2.6 | 4.2 | 2.5 | $a$=0.3555(1) | FCC | 100.0 | 90 | 2.5 | 2.5 | 2.5 | 2.5 |
| | | | | | | | Co $\varepsilon$ | 73.3 | 88.1 | 2.6 | 2.6 | 4.2 | 2.5 | $a$=0.2516(1) $c$=0.4077(3) | | | | | | | |
| E | 1373 | 18.75 | **25** | 18.75 | 18.75 | 18.75 | FCC | 100.0 | 18.7 | 25.5 | 18.7 | 18.9 | 18.2 | $a$=0.3603(1) | FCC | 100.0 | 18.75 | 25.0 | 18.75 | 18.75 | 18.75 |
| F | 1373 | 14.5 | **42** | 14.5 | 14.5 | 14.5 | FCC | 30.8 | 15.7(1) | 30.3(1) | 15.7(1) | 17.1(1) | 21.2(1) | $a$=0.3609(1) | FCC | 47.0 | 16.8 | 31.2 | 15.6 | 16.0 | 20.4 |
| | | | | | | | $\sigma$ | 69.2 | 13.8(1) | 48.3(1) | 13.9(1) | 13.0(1) | 11.0(1) | $a$=0.8817(2) $c$=0.4569(1) | BCC | 53.0 | 12.5 | 51.6 | 13.5 | 13.2 | 9.2 |
| F' | 1273 | 14.5 | **42** | 14.5 | 14.5 | 14.5 | FCC | 28.7 | 15.6(2) | 27.3(3) | 15.8(1) | 18.1(2) | 23.2(1) | $a$=0.3603(1) | FCC | 56.0 | 17.0 | 30.6 | 15.8 | 16.1 | 20.5 |
| | | | | | | | $\sigma$ | 71.3 | 13.9(1) | 48.9(1) | 14.0(1) | 12.7(1) | 10.5(1) | $a$=0.8800(1) $c$=0.4559(2) | BCC | 44.0 | 11.4 | 56.5 | 12.8 | 12.5 | 6.8 |
| G | 1373 | 7.5 | 7.5 | 7.5 | **70** | 7.5 | $\beta$ Mn | 100.0 | 7.8 | 8.0 | 7.9 | 68.5 | 7.8 | $a$=0.6307(1) | FCC | 100.0 | 7.5 | 7.5 | 7.5 | 70 | 7.5 |
| H | 1373 | 25 | 25 | 25 | 25 | - | FCC | 65.5 | 26.5(2) | 22.0(2) | 26.0(2) | 25.5(1) | - | $a$=0.3599(1) | FCC | 59.0 | 27.6 | 20.6 | 26.3 | 25.5 | - |
| | | | | | | | $\sigma$ | 35.5 | 20.7(1) | 33.7(1) | 22.1(2) | 23.5(1) | - | $a$=0.8958(4) $c$=0.4619(2) | BCC | 41.0 | 21.2 | 31.3 | 23.2 | 24.3 | - |
| H' | 1273 | 25 | 25 | 25 | 25 | - | FCC | 45.6 | 27.7(1) | 19.6(1) | 26.9(1) | 25.8(1) | - | $a$=0.3659(1) | FCC | 68.8 | 27.3 | 21.0 | 26.3 | 25.4 | - |
| | | | | | | | $\sigma$ | 54.4 | 21.1(1) | 32.8(2) | 22.4(2) | 23.7(1) | - | $a$=0.9004(1) $c$=0.4665(2) | BCC | 31.2 | 19.9 | 33.9 | 22.2 | 24.0 | - |